energies

MDPI

Article

Reduction of Structural Loads in Wind Turbines Based on an Adapted Control Strategy Concerning Online Fatigue Damage Evaluation Models

Nejra Beganovic, Jackson G. Njiri and Dirk Söffker *

Chair of Dynamics and Control, Faculty of Engineering, University of Duisburg-Essen, Lotharstraße 1-21, 47057 Duisburg, Germany; nejra.beganovic@uni-due.de (N.B.); jackson.njiri@uni.due.de (J.G.N.)

* Correspondence: soeffker@uni-due.de; Tel.: +49-(0)-203-379-3429

Received: 31 October 2018; Accepted: 3 December 2018; Published: 7 December 2018

Abstract: In recent years, the rapidly-increasing demand for energy generation from renewable resources has been noticeable. Additional requirements are consequently set on Wind Turbine (WT) systems, primarily reflected in WT size and power rating increases. With the size increase of WT, structural loads/fatigue stress on the wind turbine become larger, simultaneously leading to its accelerated aging and the shortening of its lifetime. The primary goal of this contribution is to establish an approach for structural load reduction while retaining or slightly sacrificing the power production requirements. The approach/control strategy includes knowledge about current fatigue damage and/or damage increments and consists of multi-input multi-output controllers with variable control parameters. By the appropriate selection of the designed Multi-Input Multi-Output (MIMO) controllers, the mitigation of structural loads in accordance with a predefined range of accumulated fatigue damage or damage increments, exactly to the extent required to provide a predefined service lifetime, is obtained. The validation of the aforementioned control strategy is based on the simulation results and the WT model developed by National Renewable Energy Laboratory (NREL). The obtained results prove the efficiency of the proposed control strategy with respect to the reduction of rotor blade bending moments, simultaneously exhibiting no significant impact on the resulting power generation.

Keywords: wind turbine systems; structural load reduction; online fatigue damage evaluation

1. Introduction

Energy generation from renewable sources has gained much attention in the last decade due to the drastic reduction of conventional energy sources from year to year and the rapid climate change primarily related to global warming. Among renewable energy sources, energy production from wind has been especially intensified. Concerning its growth trend, it is estimated that the installed capacity up to 2020 will reach almost 1300 TW world-wide [1,2]. Due not only to the facts that energy production using wind is recognized as environmentally friendly and is probably the most effective solution among renewable energy sources, but also due to the technological improvements achieved recently, WT systems have been brought into focus. The latest achievements are mainly focused on the development of optimal offshore solutions due to the higher potential for wind energy conversion at offshore sites in comparison with onshore installments. Offshore installments entail completely different challenges taking into consideration the difficult access to offshore sites and more complex hydrodynamical and aerodynamic loading profiles [3]. It additionally faces the problems of energy transmission (laying cables under the sea), platform design, and similar problems. However, the larger abundance and greater strength of the wind at sea compared with onshore installments are sufficient reasons to investigate the possibilities of surmounting the existing shortcomings of offshore WT systems.

Further notable improvements are the development of advanced materials used for WT fabrication or even the development of smart multi-functional structures adopting continuous Structural Health Monitoring (SHM); for instance, smart sensor and actuator grids integrated in composite structures, reinforced steel structures (nacelle), advanced data transmission facilities, and others, as mentioned in [4]. Most attention according to a number of existing publications is given to composite materials' testing and the examination of the impacts of different fabrication methodologies on the feasibility of using composites (related to changes in strength and stiffness) [5–8]. As composite materials are mainly used for WT rotor blades' fabrication and these are simultaneously the most susceptible to failure due to their direct exposure to the load, the integration of embedded sensing networks to enable continuous tracking of the state-of-health of composites is a reasonable strategy. Structural health monitoring systems implemented in such a way provide higher reliability of the system. Here, the information about the state-of-health can be used to make decisions about appropriate actions. Along with smart sensor network integration, the integration of in situ power sources in the composites has been discussed in some contributions [9–11]. Even the loading profiles (wind speed and wind direction) are variable, so power provided to the grid has to fulfill dynamic requirements [12]. To enhance the flexibility of the entire grid, integrated in situ power sources can be used to compensate lower energy production during low wind speed periods while recharging energy sources during periods of greater availability of wind. Embedding lithium-ion batteries into Carbon Fiber-Reinforced Polymers (CFRP) was proposed by Ladpli et al. [9], whereas the integration of supercapacitors in CFRP was proposed by Shirshova et al. [10]. Additional power sources utilizable for these purposes were reviewed and given in [11,13], each of them relating to different energy capacities and densities. Moreover, power generation using wind is currently more often discussed concerning wind farms, rather than individual WT systems. This additionally includes mutual relationships between individual WT systems on wind farms. It can be concluded from [4] that the benefits of smart structures are closely related to efficient SHM of WT components, at the same time making the decision about a suitable response to changing inflow conditions possible. A suitable response in this case may include the control of vibration, damping, stress distribution, and similar responses.

Regardless of the location where the WT system is installed, fluctuating structural loads that induce mechanical stress on the wind turbine to a lesser or greater extent affect the system's reliability. Due to the induced mechanical stresses, wind turbine systems and the systems' components undergo gradual degradation over time, which is related to the decreased reliability of the system. To guarantee the reliability of the WT system, reducing the asymmetric structural loads on WT blades can be considered. Through the reduction of structural loads, the predefined service lifetime by the manufacturer of the wind turbine can be extended [14].

A number of control strategies taking into consideration the mitigation of structural loads have been proposed [15–22]. In [15], the aforementioned structural loads on rotor blades were mitigated using a nonlinear Individual Pitch Control (IPC). The controller proposed in [15] consists of a "blade vibration damper and a pitch angle lead compensator" [15]. The vibration damper mitigates the blade vibrations, whilst the angle lead compensator compensates for the delay between the desired/commanded and the real pitch angle. Similarly, Houtzager et al. [16] introduced improvements to IPC by using the so-called lifted repetitive controller. The lifted repetitive controller is designed with the aim to reject load disturbances on rotor blades, leading to the reduction of structural loads and simultaneously extending the service lifetime. The results presented in [16] proved that the lifted repetitive-based control reduced the vibrations on the structure to a great extent. The use of IPC for load reduction was proposed also in [17,18]. Combined pitch and trailing edge flap control for load mitigation was proposed in [18]. The proposed control strategy included an individual pitch control loop and a trailing edge flap control loop, whereas the IPC control loop was used to mitigate the low frequency loads and the trailing edge flap control loop to mitigate the high frequency loads [18]. The control strategy proposed in [19] consisted of an optimal multivariable Linear Quadratic Gaussian (LQG) controller and a feedforward disturbance rejection controller with inaccessible wind turbine states estimated using a Kalman filter. The main objective of the LQG controller is the minimization of rotor tilt and yaw moments. The approach was

tested and compared with the conventional IPC method "in simulation studies with models of different complexities" [19]. In [20], a set of collective and individual pitch control algorithms was proposed, whereas the control algorithms were LQR control algorithms with Integral action (LQRI) utilizing Kalman filters to estimate system states. The proposed control algorithms [20] controlled rotor speed and blade bending moments at the same time. Based on the simulation results, acceptable rotor speed regulation and significant reduction of blade bending moments were achieved. Hence, a linear-quadratic regulator-based individual pitch controller aiming to reduce structural loads of wind turbines was proposed in [21].

Beside IPC, a nonlinear Model Predictive Controller (MPC) considering wind predictions was proposed for the reduction of structural loads on the WT tower and blades [23]. The information from Laser Induced Differential Absorption Radar (LIDAR) systems was used to predict wind disturbances at the front of wind turbines, which were further integrated into the control. According to [23], the use of wind predictions in this sense contributes to the mitigation of structural loads by up to 30% with almost no impact on energy production and additionally limits the pitch rates. The reduction of structural loads in the aforementioned case was achieved through the mitigation of inflow transients (gusts), which were understood as unknown disturbances to MPC. Such an implementation does not guarantee the predefined service lifetime of WT. In [23], Damage Equivalent Load (DEL) was calculated, but not integrated into the control as an online implementation of DEL calculation was not carried out. The analysis was based on a comparison of a baseline controller and MPC controller with integrated wind predictions, whereas the decrease in DEL was noticeable. Similarly, MPC was proposed in [24] to minimize the damage accumulating in the system. Improved MPC, namely a scheduled model predictive controller able to control MIMO systems with multiple control objectives, was proposed in [25]. This approach allows the introduction of system input constraints, as well as adjusting to the aerodynamic nonlinearities [25].

Active load control of wind turbine tower structural loads using the disturbance accommodating control was proposed in [26]. State-space control here was introduced to consider the coupled wind turbine dynamics. The disturbance accommodating control technique was applied to cancel the effect of wind disturbances. In a similar manner, disturbance tracking control was applied to the design of a torque controller, which optimized the energy capture under the influence of "persistent wind disturbances" [27]. In both aforementioned contributions, the mitigation of blade bending moments was reported. Disturbance accommodating-based control was also used in [28] to regulate rotor speed at above-rated wind speeds, mitigating at the same time cyclic blade root loads. Similarly, a parameterized disturbance observer-based controller with an individual pitch control strategy was designed in [29] to reduce cyclic loads generated due to wind shear and tower shadow effects. The proposed controller was able to reduce "output power fluctuation, tower oscillation and drive-train torsion" [29]. An approach to estimate the fatigue loads based on the reconstruction of data series of the stochastic properties measured at wind turbines was discussed in [30,31]. The authors here proved the possibility of accurate estimation of fatigue loads in any wind turbine on a wind farm using "only the load measurements at one single turbine and the set of wind speed measurements" [30]. For these purposes, a stochastic differential equation describing the evolution of the torque for one wind turbine driven by the wind speed was derived and used for the prediction of fatigue loads [30].

Structural loads on WT rotor blades can be reduced by appropriate WT blade design, as proposed in [32]. In accordance with this, improvements primarily in rotor blade geometry and airfoil properties ultimately affect annual energy production, the overall mass of WT, as well as WT thrust/structural loads. These three parameters are considered for optimization. It is shown that changes introduced to WT rotor blades (blade thickness, changes in chord, airfoil geometry) have a high impact on the overall performance of the WT system [32].

Although structural load mitigation of WT was discussed and achieved using different approaches in the mentioned contributions, the lack of solutions that include the information about the current state-of-health of WT and precisely-defined levels of the load that needs to be mitigated to achieve the predefined service lifetime is noticeable.

In this contribution, the evaluation of fatigue loads, targeted at integrating the knowledge about accumulated damage in the control strategy to mitigate structural loads, is given. Contrary to the aforementioned contributions, different easy to design and implement LQR-based IPC controllers and a suitable control selection module are used to achieve integration with the online estimated state-of-health and to guarantee the predefined service lifetime. The controller parameters are changed depending on the actual degradation state of WT rotor blades.

2. Model Description and Fatigue Load Evaluation

2.1. Model Description

The simulation model used in this contribution is the WindPACT1.5-MW upwind three-bladed Horizontal Axis Wind Turbine (HAWT) model developed by NREL [33]. The model has 24 Degrees of Freedom (DoFs) of which only DoFs relevant to the controller design are enabled. The DoFs enabled here are related to: top-tower fore-aft bending mode τ_f, variable generator speed mode ψ, and individual top flap-wise blade bending modes ζ_1, ζ_2, and ζ_3. The wind turbine is modeled by the nonlinear equation of motion:

$$M(\underline{q}, \underline{u}, t)\ddot{\underline{q}} + f(\underline{q}, \dot{\underline{q}}, \underline{u}, \underline{u_d}, t) = 0, \tag{1}$$

where M and f denote the mass matrix and a nonlinear function, respectively. Model control inputs are denoted as $\underline{u}$, whilst the wind profile (primarily wind speed, its stochastic nature, and present fluctuations in both inputs and outputs of the system) is denoted as $\underline{u_d}$. Component u_d as such considers also fluctuations in generated power. The enabled degrees of freedom are denoted as $\underline{q}$, whereas their velocities and accelerations are denoted as $\dot{\underline{q}}$ and $\ddot{\underline{q}}$, respectively. Five different Multi-Input Multi-Output (MIMO) controllers are designed, each of them adapted to different loading profiles. Changed loading profiles imply the change of the state-of-health indicator values (damage increments D_j or the sum of damage increments). A detailed description of the controller selection module is further given in Section 3. Each of the five different controllers is designed to provide different ratios between the power production objective and the related system's reliability; the trade-off between the aforementioned conflicting objectives is different for the five different controllers.

For controller design purposes, the model expressed by Equation (1) is linearized about different operating points. Controllers are designed in accordance with predefined nearly constant wind profiles. Due to this, five different operating points are taken into consideration, namely 14 m/s, 16 m/s, 18 m/s, 20 m/s, and 22 m/s, with a generator rotational speed of 20 rpm and pitch angles of 12.69, 16.435, 19.585, 22.289, and 24.685°, respectively. The resulting model is highly periodic due to the existence of deterministic and fluctuating load (primarily wind shear, tower deflection, and yaw misalignment). To consider model periodicity within controller design, multi-blade coordinate transformation converting the coordinates from the rotating reference frame to the non-rotating reference frame has to be done. Detailed information about multi-blade coordinate transformation is given in [33]. Finally, wind turbine representation in the state space model takes the following form:

$$\begin{aligned} \dot{x} &= Ax + Bu + B_d u_d, \\ y &= Cx + Du + D_d u. \end{aligned} \tag{2}$$

Here, state space vector x is represented as $x = [\Delta q, \Delta \dot{q}]^T$ and the control input as $u = [\Delta\beta_1, \Delta\beta_2, \Delta\beta_3]^T$. Matrices A, B, C, D, and D_d denote the model system matrix, the control input and output matrix, the disturbance input matrix, and the disturbance transmission matrix, respectively. The state space model given by Equation (2) is used for the control design.

2.2. Fatigue Evaluation and Controller Selection Module

As stated in the previous section, five different controllers are designed with respect to different loading profiles. Each of them realizes a different level of structural load reduction. The induced

structural loads taking into consideration different loading profiles are different. Higher structural loads lead accordingly to higher related damage contribution. The main objective concerned in controller design is to ensure the control of structural loads along with the desired objective related to power production.

Due to the SoHcalculation with respect to the Remaining Useful Lifetime (RUL), the lifetime itself becomes controllable. Briefly speaking, two control levels are combined: (i) WT control as the primary control and (ii) lifetime control as the secondary control. Lifetime control is realized through a simple calculation regarding the desired lifetime; the achieved SoH and resulting RUL, affecting thereby the primary control level. In the first case, the knowledge about overall damage accumulated in the system is used to select one of five designed controllers, implying that the selection is based on reaching threshold levels of accumulated damage. In the second case, controller selection is based solely on information about the damage increments. This means that only the information about the rate of change in accumulated damage at a particular moment is concerned. Results obtained using controller selection based on information about overall damage or damage increments in the two aforementioned cases are compared, targeting at revealing the efficiency of the proposed control strategy.

The calculation of damage increments and resulting overall damage in the system is carried out by using the Palmgren–Miner damage accumulation rule and the online Rainflow Counting Algorithm (RCA). RCA in its original form cannot be applied here, as it assumes knowledge about arbitrary loads over the complete service lifetime and is therefore not intended for online implementation [34]. Further, offline implementation is useful neither in real-time systems, nor in simulation models, where control inputs are affected by outputs from RCA. The output of the controller module (including five controllers and the controller selection module) is affected by the output of RCA, so an online RCA implementation is required. In this contribution, an implementation of the online RCA proposed by Musallam et al. [34] is employed. Such an implementation of RCA does not require tracking of complete time-history data (here, structural loads) to obtain equivalent half- and full-loading cycles. The above-mentioned algorithm processes each extremal value (minimum and maximum) at the time of their occurrence, as depicted in Figure 1. Equivalent half and full cycles generated using online RCA are further integrated in the Palmgren–Miner damage accumulation rule to calculate the Remaining Useful Lifetime (RUL) under the assumption of a known predefined service lifetime given by the manufacturer. The wind turbine predefined service lifetime is assumed as 20 years.

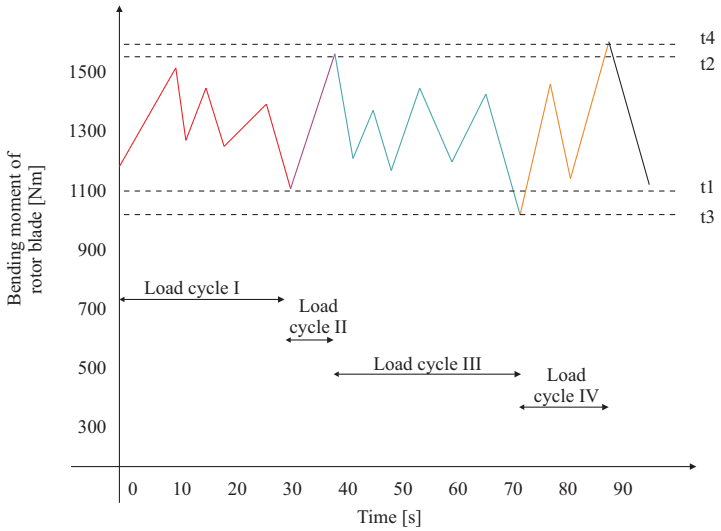

Figure 1. Graphical representation for the online implementation of Rainflow Counting Algorithm (RCA) (here: different colors represent crossing extremal values t1, t2, t3, and t4) [21].

The calculation of the damage increments and accumulated damage using the Palmgren–Miner rule is given by:

$$D_j = \sum_{i=1}^{j} d_i = \sum_{i=1}^{j} \frac{n_i}{N_i}, \tag{3}$$

where n_i denotes the number of half or full cycles corresponding to the i_{th}stress level, N_i denotes the number of cycles until failure, and D_j refers to the accumulated damage.

It is important to emphasize that no run-to-failure data are used for RUL calculation. Here, cycles are understood as the individual load units. On the contrary, representative time-series data of flap-wise bending moments of rotor blades corresponding to 600 s of simulation time are chosen as the input in RCA. Using the considered dataset, damage increments up to the predefined failure are extrapolated. In this contribution, the applied load is composed of a repetition of 600-s loading profile elements. This includes, without loss of generality, in combination with the different controllers (levels), the resulting damage increments that can be calculated and are therefore considered as known.

As the input to the fatigue damage evaluation module, any of the fatigue-equivalent variables (measurements) can be utilized: flap- and edge-wise bending moments of blades, tower fore-aft deflection of the tower, or side-to-side bending moment. The analysis is limited to the examination of RUL estimation using flap-wise bending moments of rotor blades and is chosen as the input to the fatigue damage accumulation module.

3. Controller Design

It is important to emphasize that the model of WT is provided by NREL. For controller design, it is important to determine which inputs and outputs are of high importance in terms of controller objectives and load mitigation. Simulation parameters, as well as the wind profile used for simulation are transferred to the model through configuration files provided by NREL, whereas also, the sampling rate is defined. Determined inputs and outputs in this case are closely related to enabled DoFs, which are explained in detail in Section 2.1 and shown in Figure 2.

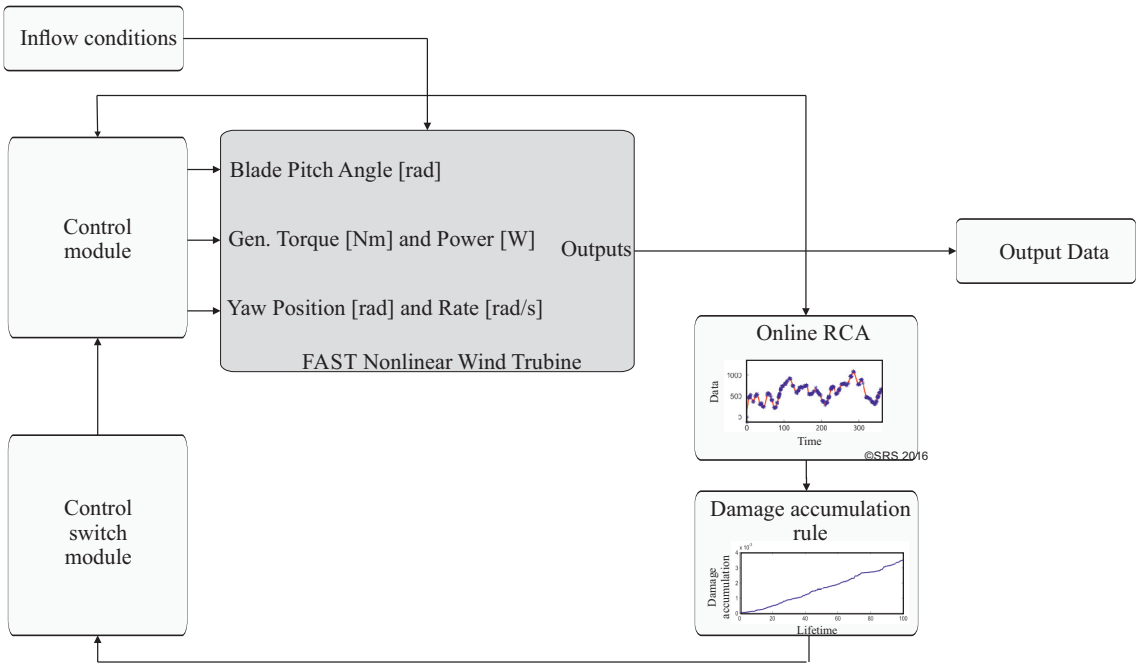

Figure 2. Proposed control strategy.

Five controllers are designed, affecting structural loads to a greater or lesser extent depending on the loading profile and accompanying damage increments, whilst generator power and rotor speed have to be maintained as close as possible to the desired values. To provide the control of generator

power and rotor speed, a baseline PI controller is used, but is not further elaborated here. Additionally, individual blade pitch (IPC) controllers are proposed for the reduction of flap-wise rotor blade bending moments [35]. Individual blade pitch controllers are designed as LQR-based controllers. As introduced in detail in [35], the objective function to be minimized is expressed as:

$$J = \int_0^t \left(x^T Q x + u^T R u \right) dt, \tag{4}$$

where u is the control input and x denotes the system state variable, while Q and R are the state and control weighting matrices, respectively. Here, Q optimizes the trade-off between power/speed regulation and structural load reduction. On the other hand, R is used to penalize the control efforts.

The tuning of controllers includes the selection of suitable Q and R matrices corresponding to different levels of structural load reduction. Not all system states are directly accessible, implying the utilization of the Kalman filter to estimate the inaccessible system states. The linearized model introduced in Section 2.1 is used to design the controllers. The complete control scheme with integrated fatigue load examination is depicted in Figure 2. Inputs to the control module according to Figure 2 are, besides measured or estimated system variables, estimated damage increments or accumulated damage over time (depending on the considered case).

4. Simulation Results

The results obtained under the usage of the fatigue damage evaluation model along with controller selection based on information about the damage accumulated over the service lifetime are depicted in Figures 3 and 4. Similarly, the results obtained using controller selection based solely on information about damage increments are given in Figures 5 and 6.

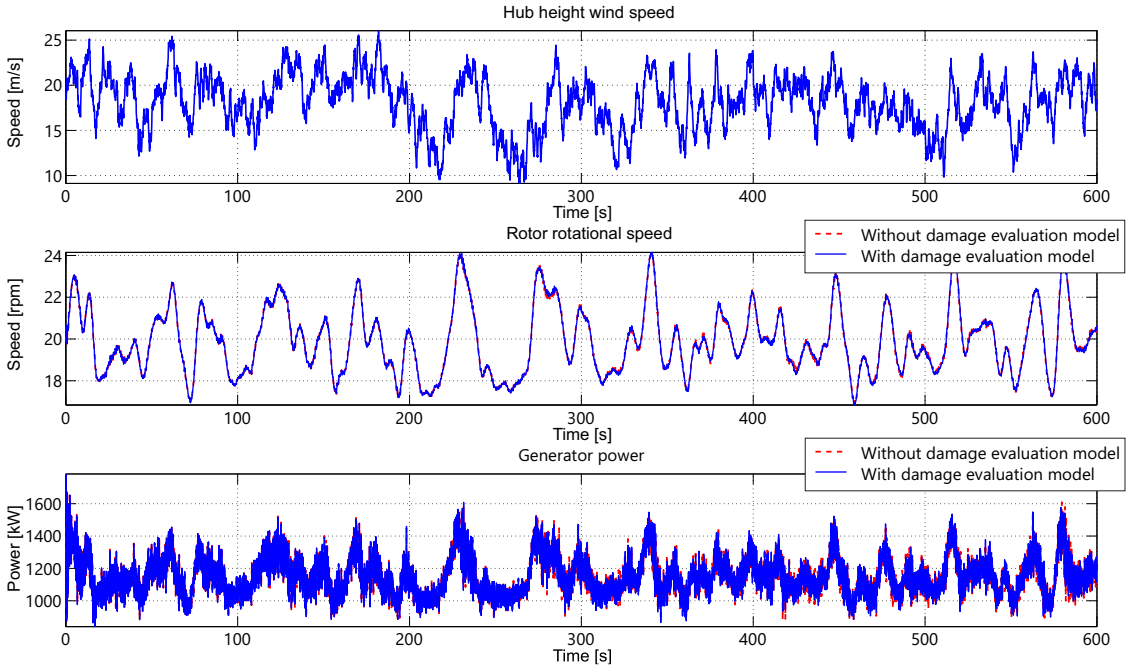

Figure 3. *Cont.*

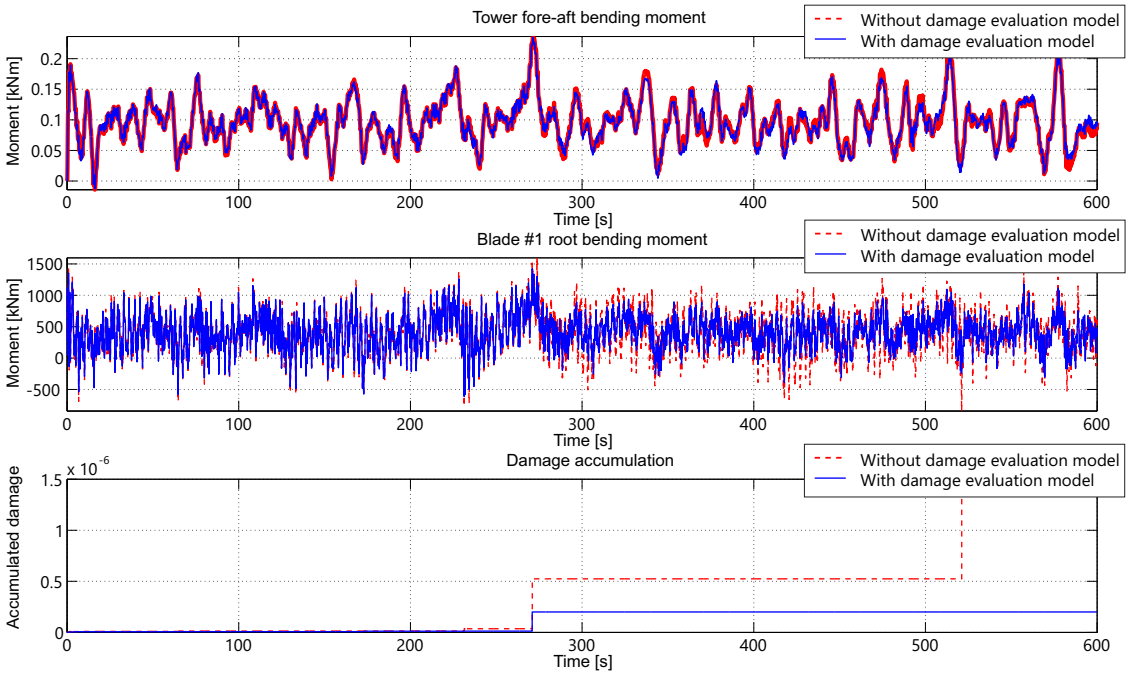

Figure 3. Simulation results concerning controller selection using the information about accumulated damage (Part I).

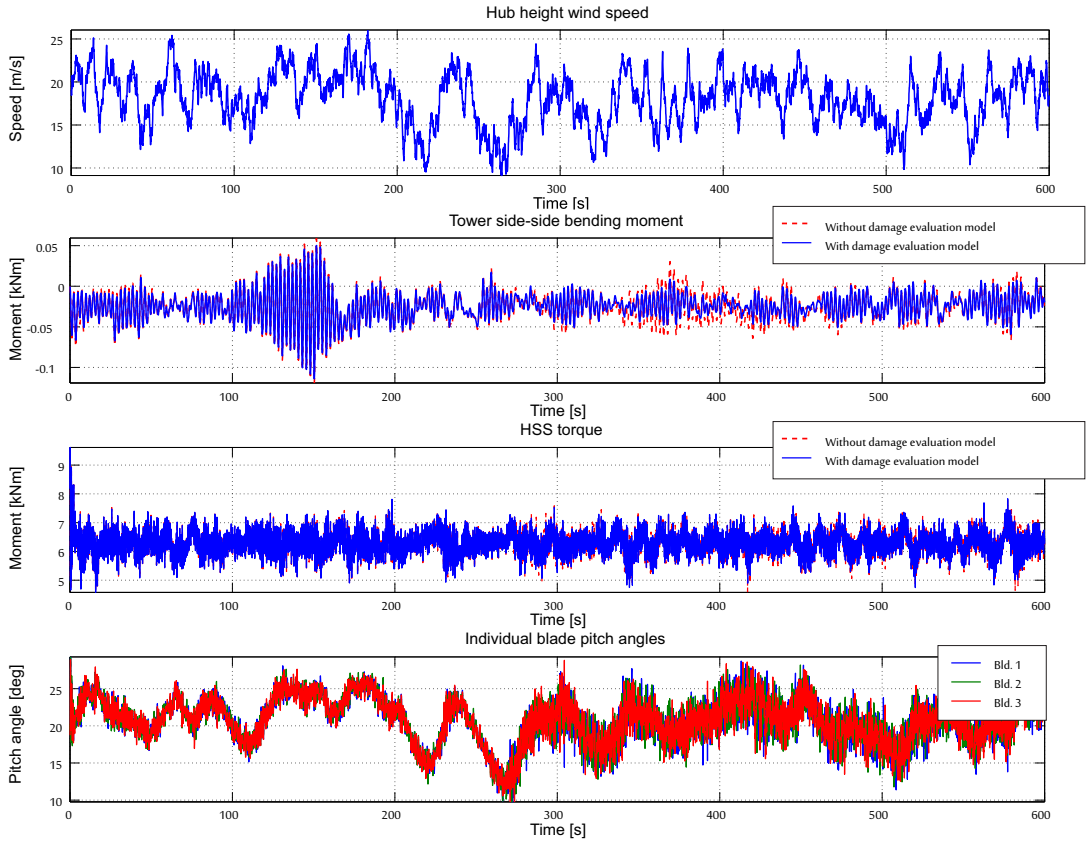

Figure 4. Simulation results concerning controller selection using the information about accumulated damage (Part II).

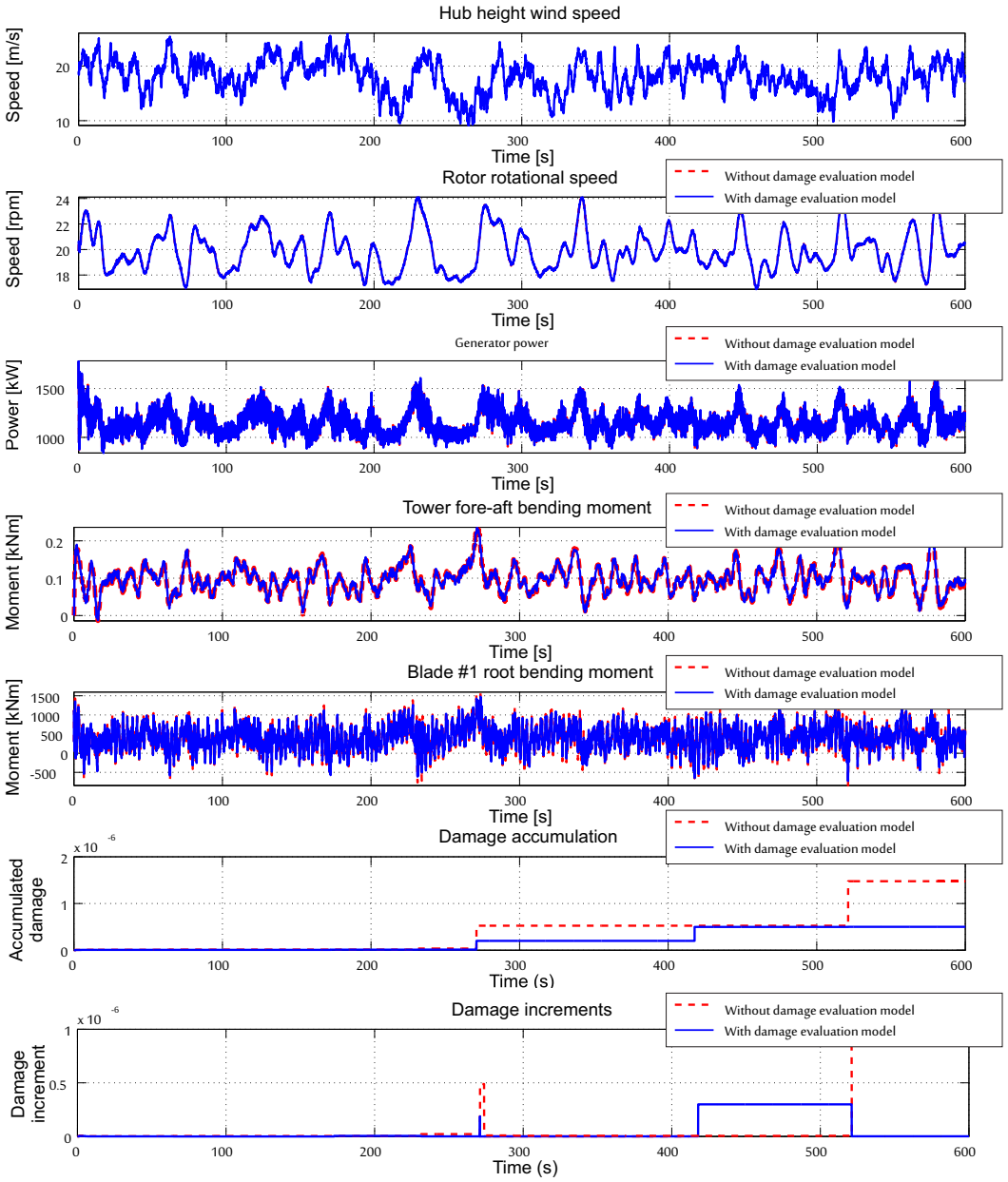

Figure 5. Simulation results concerning controller selection using only the information about damage increments (Part I).

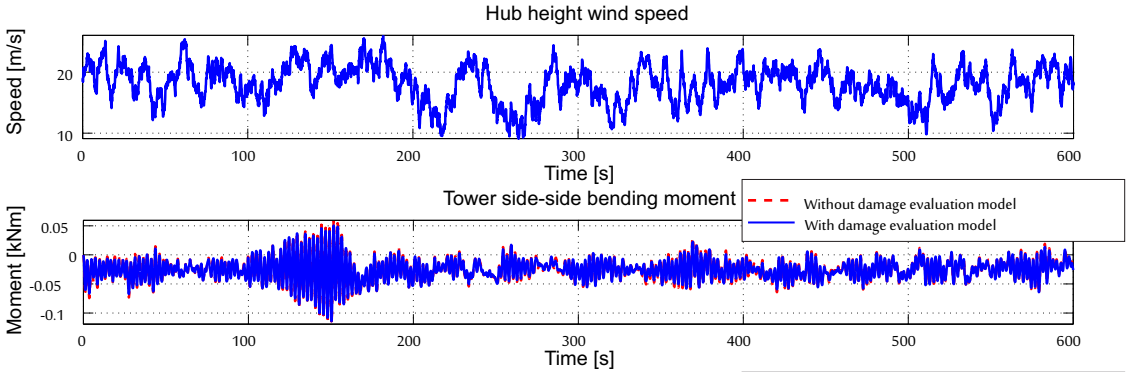

Figure 6. *Cont.*

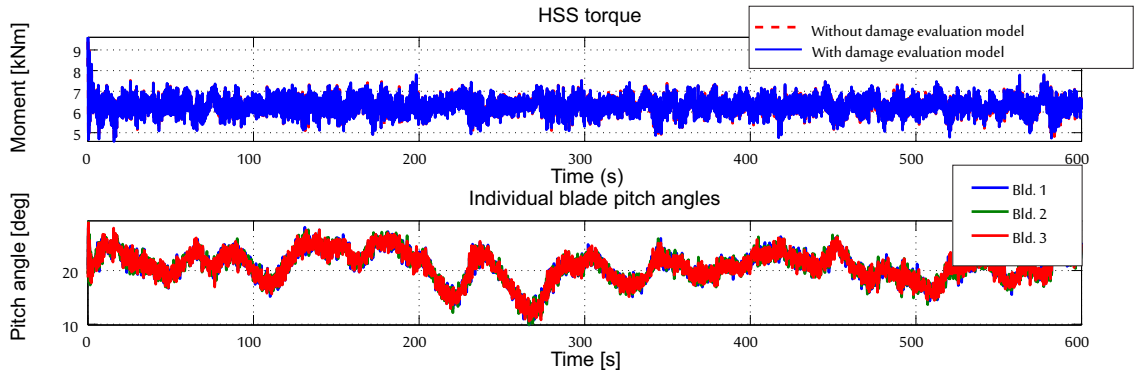

Figure 6. Simulation results concerning controller selection using only the information about damage increments (Part II).

In the upper diagrams of Figures 3–6, wind speed at hub height, serving as one input to the wind turbine model, is given beside the controller outputs. Relevant system variables to be monitored are the generator power and rotor rotational speed. Here, no significant impact on generator power and rotor rotational speed was noticeable as the sacrifice of generator power/rotor rotational speed has to be in acceptable limits. Besides these two system variables, the root bending moment of Blade #1, fore-aft bending moment of the tower, as well as the accumulated damage are depicted in the lower diagrams in Figures 3 and 5. Additionally, the effect of the adopted control strategy on the tower side-to-side bending moment, as well as high-speed shaft torque is illustrated in Figures 4 and 6. The accumulated damage and accompanying damage increments (for the case where controller selection is done solely based on tracking damage increments) are given in Figures 3 and 5. Controller #1 is the controller that provides the lowest impact on structural load reduction, whilst Controller #5 is that with the highest one.

Discussion about the Results Obtained

At first glance, it can be noticed that the level of flap-wise bending moment reduction (here, Blade #1) was much higher concerning controller selection based on accumulated damage than it was in the case when a particular controller was chosen based exclusively on information about the damage increments.

This result can be explained by the fact that in the case of controller selection based solely on the values of damage increments, the previously accumulated damage was not considered. Otherwise, it would be considered that the previous loading profile had no impact on damage accumulation and the consequent aging of system, but was still usable for the examination of structural loads in a short time framework. As such, the controller with the best performance regarding the reduction of structural loads was chosen only when the damage increment became very high. Accordingly, with the decrease of the damage increment, the controller with the worst performance according to the reduction of structural loads was chosen.

From another point of view, if values of damage increments were considered along with the overall damage accumulated in the system, then the controller with the best performance according to the reduction of structural loads was chosen as the system approached the end of its lifetime. This means that the highest level of the reduction of structural loads was achieved shortly before the end of the lifetime, albeit at a slightly compromised speed/power production objective. This caused the selection of the controller to be carried out in a successive way, and the controller with a higher level of structural load reduction, once chosen, was never swapped with a controller providing a lower level of structural load reduction.

Moreover, the tower side-side bending moment, as well as tower fore-aft bending moments were slightly decreased, even if the controllers were not designed to consider the reduction of the bending moments of the tower. As depicted in Figures 3 and 4, the generator power and generator rotational speed were in both cases slightly scarified; but to a lesser extent, so that the decrease in

power production was still acceptable. It is worth emphasizing that the controller with the highest impact on structural load reduction (Controller #5) produced in general a higher deviation between the desired and actual power generation. Exactly this fact justifies the integration of fatigue load examination in the control module, so that the sacrifice of power generation is acceptable in the case that the RUL of its lifetime is decreased to a predefined level.

The results presented in Section 4 are compliant with the desired optimization goal, which is the determination of the trade-off between energy production and WT reliability. As such, the proposed control strategy can be considered as efficient.

The resulting dependence and effects between rotor bending moment and generated power are depicted in Figures 7 and 8. The dependence between High-Speed Shaft (HSS) torque and generated power is shown in Figures 9 and 10.

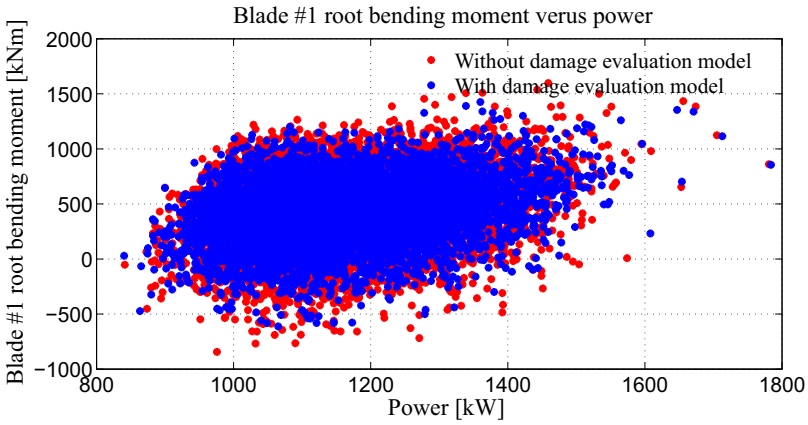

Figure 7. The change of the rotor bending moment depending on the power with the controller selection using the information about the accumulated damage.

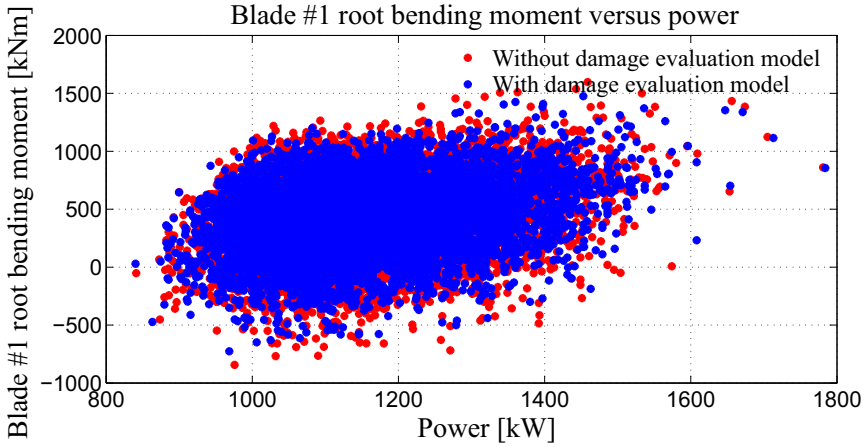

Figure 8. The change of the rotor bending moment depending on the power with the controller selection using only the information about the damage increments.

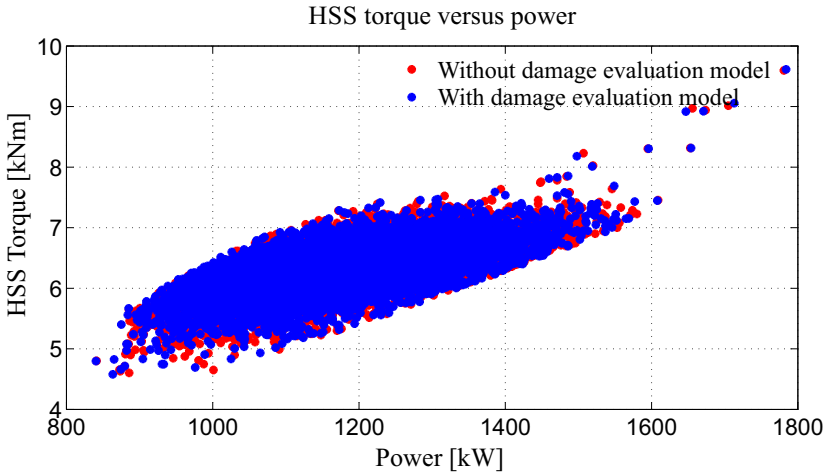

Figure 9. The change of HSS torque depending on the power with the controller selection using the information about the accumulated damage.

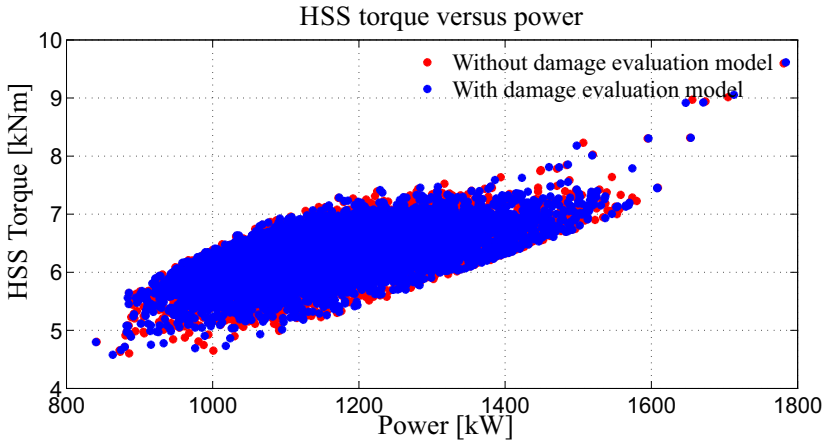

Figure 10. The change of the HSS torque in depending on the power with the controller selection using only the information about the damage increments.

The control results based on the use of the accumulated damage are depicted in Figures 7 and 9, whilst the control results based on the actual resulting damage increments are shown in Figures 8 and 10. Such a graphical illustration of the results obtained was used here to evaluate the performance of the newly-developed control strategy.

According to the results presented, a high impact on the flap-wise rotor blade bending moment was noticeable. The result of the implemented mechanism becomes clear in Figures 7 and 8. The control reduced the number of outliers strongly affecting the lifetime, but the overall behavior was not effected. At the same time, the reduction of the high-speed shaft torque was much less. This implies that the reduction of structural loads on rotor blades did not have a high impact on HSS torque. This proves the capability of the proposed control strategy to reduce structural loads on WT blades without a significant impact on HSS torque. In addition, the standard deviation of generated power, HSS torque, and Blade #1 root bending moment are calculated and presented in Table 1 to show not only qualitative, but also quantitative indicators.

Table 1. Values of the standard deviation.

	Generated Power	HSS Torque	Blade #1 Root Bending Moment
Case I	177.8914	0.9057	494.5175
Case II	176.9045	0.9004	479.5804
Case III	177.2104	0.9041	482.5486

All cases depicted in Figures 9 and 8 were analyzed. Three cases are stated in Table 1 as: (i) Case I, the model without structural load reduction consideration: the baseline PI controller; (ii) Case II, the model with the consideration of structural load reduction: controller selection based on accumulated damage; and (iii) Case III, the model with the consideration of structural load reduction: controller selection based on damage increments. However, the same conclusion was made, as the highest discrepancy in the standard deviation was obtained for bending moments, whilst the same did not change to a great extent for HSS torque and generated power.

5. Summary and Conclusions

In this contribution, a new control strategy for WT systems is introduced. The developed control strategy provides a trade-off between the mitigation of structural loads and the desired power production. By the evaluation of fatigue loads and the appropriate adoption of the control strategy according to the examined fatigue loads, it was intended to achieve the mitigation of structural loads. For this purpose, five different MIMO controllers corresponding to different levels of structural load reduction were designed. All MIMO controllers were LQR-based controllers, where the adjustment of the level of structural load reduction was obtained by appropriate selection of the Q and R matrices. Moreover, the usage of a number of MIMO controllers is equivalent to the usage of a single controller with adaptive controller parameters. The selection of a particular MIMO controller was conditioned by the actual value of damage accumulation or the damage increment, which were calculated using an appropriate fatigue damage evaluation model.

The results obtained prove that the proposed control strategy enabled the reduction of structural loads in combination with a slight compromise on the power generation. The mitigation of structural loads was analyzed using (i) successive controller selection, whereas the MIMO controller providing the highest level of structural load reduction corresponded to the highest values of accumulated damage, or (ii) damage increment-conditioned controller selection, whereas the MIMO controller providing the highest level of structural load reduction corresponded to the highest values of damage increments. In the case that the controller selection was carried out using accumulated damage, the reduction of structural loads was higher as the system was closer to its end of lifetime. On the contrary, in the case that the controller selection was conditioned by the tracking of damage increments, the reduction of structural loads had a short time span with a noticeable change of the structural loads.

This approach implicitly assumed that the damage between two subsequent load cycles stays constant. As this case rarely occurs in practice, the development of additional fatigue damage evaluation models can be investigated in the future to obtain a more accurate prediction of RUL. Besides the development of improved fatigue damage accumulation models, further improvements are still possible concerning the control strategy. These improvements may lead to an investigation of the possibilities to consider the mitigation of other structural loads of WT along with rotor blade structural loads, such as top-tower fore-aft and top-tower side-to-side tower structural loads.

Author Contributions: All authors contributed equally to the contribution. N.B. was to the highest extent responsible for the draft version preparation, figures, and literature research. J.G.N. and D.S. were mainly responsible for the organization and structure definition and provided the initial review of the contribution. D.S. introduced ideas, suggested the organization of the work, and was also responsible for proofreading.

Funding: The APC was funded by the Open Access Publication Fund of the University of Duisburg-Essen. The research was funded by German Academic Exchange Service.

Acknowledgments: Support by the Open Access Publication Fund of the University of Duisburg-Essen and German Academic Exchange Service is gratefully acknowledged.

Conflicts of Interest: The authors declare no conflict of interest.

Abbreviations

The following abbreviations are used in this manuscript:

WT	Wind Turbine
MIMO	Multi-Input Multi-Output
NREL	National Renewable Energy Laboratory
SHM	Structural Health Monitoring
CFRP	Carbon Fiber-Reinforced Polymers
MES	Multifunctional Energy Storage composites
MPC	Model Predictive Controller
DEL	Damage Equivalent Load
IPC	Individual blade Pitch Controller
HSS	High-Speed Shaft
DoF	Degree of Freedom
LQG	Linear Quadratic Gaussian
RUL	Remaining Useful Lifetime
RCA	Rainflow Counting Algorithm
LIDAR	Laser Induced Differential Absorption Radar
HAWT	Horizontal Axis Wind Turbine

References

1. Sawyer, S.; Teske, S.; Rave, K.; Global Wind Energy Council (GWEC). *Global Wind Energy Outlook 2014*; Tech. Report; GWEC: Brussels, Belgium, 2014.
2. Wang, P.; Gao, Z.; Bertling, L. Operational adequacy studies of power systems with wind farms and energy storages. *IEEE Trans. Power Syst.* **2012**, *27*, 2377–2384. [CrossRef]
3. Perveen, R.; Kishor, N.; Mohanty, S.R. Off-shore wind farm development: Present status and challenges. *Renew. Sustain. Energy Rev.* **2014**, *29*, 780–792. [CrossRef]
4. Chopra, I. Review of state of art of smart structures and integrated systems. *AIAA J.* **2002**, *40*, 2145–2187. [CrossRef]
5. Yang, Y.; Boom, R.; Irion, B.; van Heerden, D.J.; Kuiper, P.; de Wit, H. Recycling of composite materials. *Chem. Eng. Process. Process Intensif.* **2012**, *51*, 53–68. [CrossRef]
6. Sobczak, J.J.; Drenchev, L. Metallic functionally graded materials: A specific class of advanced composites. *J. Mater. Sci. Technol.* **2013**, *29*, 297–316. [CrossRef]
7. Dandekar, C.R.; Shin, Y.C. Modeling of machining of composite materials: A review. *Int. J. Mach. Tools Manuf.* **2012**, *57*, 102–121. [CrossRef]
8. Koronis, G.; Silva, A.; Fontul, M. Green composites: A review of adequate materials for automotive applications. *Compos. Part B Eng.* **2013**, *44*, 120–127. [CrossRef]
9. Ladpli, P.; Nardari, R.; Wang, Y.; Hernandez-Gallegos, P.A.; Rewari, R.; Kuo, H.T.; Kopsaftopoulos, F.; Chang, F.K. Multifunctional Energy Storage Composites for SHM Distributed Sensor Networks. *Struct. Health Monit.* **2015**, *2*, 2217–2227.
10. Shirshova, N.; Qian, H.; Shaffer, M.; Steinke, J.; Greenhalgh, E.; Curtis, P.; Kucernak, A.; Bismarck, A. Structural composite supercapacitors. *Compos. Part A Appl. Sci. Manuf.* **2013**, *46*, 96–107. [CrossRef]
11. Zhao, H.; Wu, Q.; Hu, S.; Xu, H.; Rasmussen, C.N. Review of energy storage system for wind power integration support. *Appl. Energy* **2015**, *137*, 545–553. [CrossRef]
12. Akintayo, A.; Zhou, W. Assessment and Performance Evaluation of a Wind Turbine Power Output. *Energies* **2018**, *11*, 1992.
13. Liu, P.; Sherman, E.; Jacobsen, A. Design and fabrication of multifunctional structural batteries. *J. Power Sources* **2009**, *189*, 646–650. [CrossRef]
14. Vesel, R.W.; McNamara, J.J. Performance enhancement and load reduction of a 5 MW wind turbine blade. *Renew. Energy* **2014**, *66*, 391–401. [CrossRef]
15. Wentao, Y.; Hua, G.; Shuai, X.; Geng, Y. Nonlinear individual pitch control of large wind turbines for blade load reduction. In Proceedings of the International Conference on Renewable Power Generation, Palermo, Italy, 22–25 November 2015; pp. 1–6.

16. Houtzager, I.; van Wingerden, J.W.; Verhaegen, M. Wind turbine load reduction by rejecting the periodic load disturbances. *Wind Energy* **2013**, *16*, 235–256. [CrossRef]
17. Bossanyi, E.A. Further load reductions with individual pitch control. *Wind Energy* **2005**, *8*, 481–485. [CrossRef]
18. He, K.; Qi, L.; Zheng, L.; Chen, Y. Combined Pitch and Trailing Edge Flap Control for Load Mitigation of Wind Turbines. *Energies* **2018**, *11*, 2519. [CrossRef]
19. Selvam, K.; Kanev, S.; van Wingerden, J.W.; van Engelen, T.G.; Verhaegen, M. Feedback-feedforward individual pitch control for wind turbine load reduction. *Int. J. Robust Nonlinear Control* **2009**, *19*, 72–91. [CrossRef]
20. Park, S.; Nam, Y. Two LQRI based blade pitch controls for wind turbines. *Energies* **2012**, *5*, 1998–2016. [CrossRef]
21. Njiri, J.G.; Beganovic, N.; Mahn, H.M.; Söffker, D. Consideration of lifetime and fatigue load in wind turbine control. *Renew. Energy* **2019**, *131*, 818–828. [CrossRef]
22. Lackner, M.A. An investigation of variable power collective pitch control for load mitigation of floating offshore wind turbines. *Wind Energy* **2013**, *16*, 435–44. [CrossRef]
23. Schlipf, D.; Schlipf, D.J.; Kühn, M. Nonlinear model predictive control of wind turbines using LIDAR. *Wind Energy* **2013**, *16*, 1107–1129. [CrossRef]
24. Sanchez, H.; Escobet, T.; Puig, V.; Odgaard, P.F. Health-aware model predictive control of wind turbines using fatigue prognosis. *IFAC-PapersOnLine* **2015**, *48*, 1363–1368. [CrossRef]
25. Kumar, A.; Stol, K. Scheduled model predictive control of a wind turbine. In Proceedings of the 47th AIAA Aerospace Sciences Meeting Including the New Horizons Forum and Aerospace Exposition, Orlando, FL, USA, 22–25 November 2009; pp. 481–498.
26. Menezes, E.J.N.; Araujo, A.M.; Rohatgi, J.S.; del Foyo, P.M.G. Active load control of large wind turbines using state-space methods and disturbance accommodating control. *Energy* **2018**, *150*, 310–319. [CrossRef]
27. Stol, K.A. Disturbance tracking control and blade load mitigation for variable-speed wind turbines. *J. Sol. Energy Eng.* **2003**, *125*, 396–401. [CrossRef]
28. Stol, K.A.; Balas, M.J. Periodic disturbance accommodating control for blade load mitigation in wind turbines. *J. Sol. Energy Eng.* **2003**, *125*, 379–85. [CrossRef]
29. Imran, R.M.; Hussain, D.M.; Chowdhry, B.S. Parameterized Disturbance Observer Based Controller to Reduce Cyclic Loads of Wind Turbine. *Energies* **2018**, *11*, 1296. [CrossRef]
30. Lind, P.G.; Herráez, I.; Wächter, M.; Peinke, J. Fatigue load estimation through a simple stochastic model. *Energies* **2014**, *7*, 8279–8293. [CrossRef]
31. Lind, P.G.; Vera-Tudela, L.; Wächter, M.; Kühn, M.; Peinke, J. Normal Behaviour Models for Wind Turbine Vibrations: Comparison of Neural Networks and a Stochastic Approach. *Energies* **2017**, *10*, 1944. [CrossRef]
32. Fischer, G.R.; Kipouros, T.; Savill, A.M. Multi-objective optimization of horizontal axis wind turbine structure and energy production using aerofoil and blade properties as design variables. *Renew. Energy* **2014**, *62*, 506–515. [CrossRef]
33. Bir, G.S. *User's Guide to MBC3: Multi-Blade Coordinate Transformation Code for 3-Bladed Wind Turbines*; Tech. Report; National Renewable Energy Laboratory (NREL): Golden, CO, USA, 2008.
34. Musallam, M.; Johnson, C.M. An efficient implementation of the Rainflow Counting Algorithm for life consumption estimation. *IEEE Trans. Reliab.* **2012**, *61*, 978–986. [CrossRef]
35. Njiri, J.G.; Liu, Y.; Söffker, D. Multivariable Control of Large Variable-Speed Wind Turbines for Generator Power Regulation and Load Reduction. *IFAC-PapersOnLine* **2015**, *48*, 544–549. [CrossRef]